High-resolution positron scattering from helium: Grand total and positronium-formation cross sections

P. Caradonna, A. Jones, C. Makochekanwa, D. S. Slaughter, J. P. Sullivan, and S. J. Buckman*
ARC Centre for Antimatter-Matter Studies, Research School of Physics and Engineering, Australian National University, Canberra, Australian Capital Territory 0200, Australia

I. Bray and D. V. Fursa
ARC Centre for Antimatter-Matter Studies, Curtin University of Technology, GPO Box U1987, Perth, Western Australia 6845, Australia
(Received 26 June 2009; published 22 September 2009)

Measurements of the grand total and positronium-formation cross sections for positrons scattered by helium within the impact energy range from 10 to 60 eV are presented. All measurements presented here use a high-resolution (~70 meV) trap-based pulsed positron beam. Scattering is studied using a high-magnetic field, and absolute measurements of the scattering cross sections are obtained without the need for normalization to other cross sections. We also present single center, convergent close coupling calculations of the total cross section. A detailed study of the cross section to investigate the possibility of scattering resonances and channel coupling has been made. Comparisons with previous cross-section measurements and theoretical calculations are also included.

DOI: 10.1103/PhysRevA.80.032710 PACS number(s): 34.80.Uv, 34.80.Lx, 34.80.Bm

I. INTRODUCTION

Fundamental differences emerge when one compares cross sections for positron scattering by atoms or molecules with those for electron collisions, particularly at low-impact energies, and even at the grand total cross-section level. These differences are due to a number of factors. Since the charge of the positron is opposite to that of the electron, the positron experiences a net repulsion by the mean static potential and as positrons are distinguishable from electrons, they do not undergo exchange processes. A further key difference between these projectiles is that positrons can undergo annihilation and/or positronium (Ps) formation with bound electrons. Positronium, a temporary bound state, which can form when a positron picks off an atomic or molecular electron, is a very strong scattering channel and it contributes a major portion of the grand total cross section at low-impact energies. As a result of these differences, the study of low-energy interactions between positrons and atoms or molecules provides an important additional test for contemporary quantum collision theories.

From an experimental point of view, positron collision physics is much less advanced when compared to its electron counterpart, particularly at low-impact energies. Progress has been hindered by difficulties with positron source technology that limit flux and energy resolution. Nonetheless, there are many examples of significant advances in the field over the past 20 years or so [1]. In recent years, the advances, which have been made with buffer-gas trapping of positrons have also made available new methods for the study of positron scattering. The present work represents the first time that these techniques [2–4] have been applied to the study of positron interactions with the helium atom.

Helium is an important target as it is the simplest, fundamental atomic system for testing and improving our experimental and theoretical techniques. In the case of positron interactions, it is likely that the helium atom could provide a useful test bed for theoretical calculations with regard to how the Ps formation channel can be accurately described in a general scattering calculation.

There have been many previous measurements of the grand total cross section for positron scattering from helium below 60 eV [5–10] and references therein. All previous measurements have used positron beams with energy resolutions of 0.1 eV or greater, although this has not been a barrier to establishing a benchmark value for scattering below the positronium formation threshold at 17.8 eV [5]. The primary goal of the present work is to provide benchmark measurements of both the total and positronium-formation cross sections at energies up to 60 eV, and to use these to both test and guide theory [11].

II. APPARATUS AND TECHNIQUES

The experimental apparatus used for these measurements is based on the Surko buffer-gas trap system, developed at University of California at San Diego (UCSD) [2,3]. It has been comprehensively described elsewhere [12] and so only a brief overview of the operation will be presented here.

Positrons are obtained from a radioactive ^{22}Na source, with a strength of approximately 30 mCi for the measurements described in this paper. A solid neon moderator is used to form a low-energy positron beam with an energy width of approximately 1.5 eV. Using electrostatic and solenoidial magnetic fields, these moderated positrons are guided from the source into the buffer-gas trap.

The trap electrodes are configured to form stepped, electrostatic potential wells, and positrons confined in these wells lose energy rapidly through inelastic collisions with N_2 and CF_4 buffer gases. They are confined in the trap and quickly thermalize to the buffer gas temperature. Positrons are released from the trap by modulating the potential on one of

*stephen.buckman@anu.edu.au

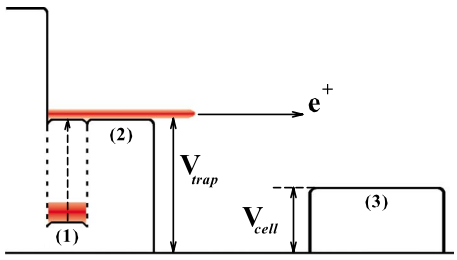

FIG. 1. (Color online) The solid lines are a schematic representation of the potentials applied to the latter part of the trap and cell electrodes; (1) dump, (2) exit gate (V_{trap}), and (3) gas cell (V_{cell}) electrodes.

the final electrodes, see Fig. 1, such that a pulsed beam, with between 300 to 500 positrons per pulse is formed. The energy distribution of positrons in this cooled sample is measured downstream using a retarding potential analyzer (RPA) and typically it is around 60–75 meV.

The trap typically cycles at 200 Hz and the positrons exiting the trap are electrostatically and magnetically guided into a 200 mm long cylindrical gas cell with an internal diameter of 76 mm and with 5 mm end apertures. The schematic in Fig. 1 shows that the energy of the incident positrons (E_{in}) through the gas-cell region is equal to,

$$E_{in} = e(V_{trap} - V_{cell}) \tag{1}$$

the difference between the electrode potential set at the exit gate of the trap (V_{trap}) and the gas cell (V_{cell}).

Helium is continuously fed into the center of the gas cell and is differentially pumped out at both ends using two turbomolecular pumps. This sets up a well defined, higher gas pressure through the scattering cell region so that the scattering length can be taken to be 200 mm, the length of the gas cell [12]. The pressure was set to avoid the possibility of multiple scattering effects, and this was checked by performing pressure dependence measurements of the cross section. All positrons that exit the gas cell are magnetically and electrostatically guided through a RPA which analyzes only the energy component of the beam ($E_{\|}$), which is parallel to the axial magnetic field [4]. Only those positrons whose values of ($E_{\|}/e$) are above the potential set at the RPA can pass through and be detected by a double-stack microchannel plate (MCP). The collected current is amplified using a charge-sensitive preamp and the data stored by the experimental control computer.

An extensive discussion of the derivation of the cross sections for positron scattering in a strong magnetic field has been reported elsewhere [1,4]. Figure 2 is a schematic of a normalized RPA intensity spectrum as a function of retarding voltage that can be obtained for an impact energy of 33 eV.

Since the incident intensity (I_o) is attenuated by the target gas, particular care must be taken if all the incident positrons are to be detected. This is achieved by setting the RPA potential to 0 V and choosing a potential at the gas cell (V_{cell}), such that $0 < E_{in} \ll 17.8$ eV. In this case, E_{in} falls well below the energy required to form Ps, so no loss of incident positrons due to Ps formation can occur. Since scattering takes place in a 530 G uniform magnetic field region, all the incident positrons passing through the gas cell, with the exception of those scattered into a small region near 90°, will reach the MCP and be detected.

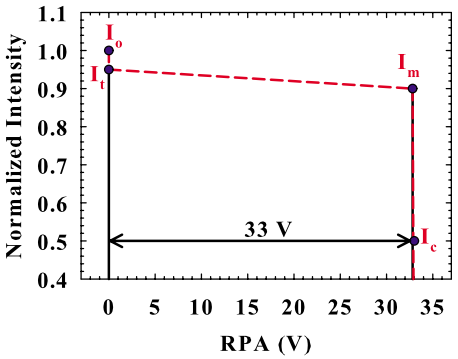

FIG. 2. (Color online) RPA data for a 33 eV positron scattered by helium (●). I_c=0.5 corresponds to the cutoff potential.

The transmitted intensity (I_t), which has lost some portion of positrons due to the formation of Ps, is measured by setting the potential at the gas cell and RPA to 0 V (E_{in} =33 eV). The transmitted intensity that contains only the unscattered portion of incident positrons (I_m) is measured by keeping E_{in}=33 eV, while raising the potential at the RPA to $\approx V_{trap}$.

The cross sections for various processes can then be experimentally determined using the Beer Lambert law, Eq. (2), where (n) is the gas number density, (l) is the path length through the gas, and (F) is the appropriate fraction of measured intensities, for a given process.

$$\sigma = -\frac{1}{nl}\ln(F). \tag{2}$$

For the present experiment, the quantity $F=I_m/I_o$, in Eq. (2), would be the scattering fraction needed to experimentally calculate the grand total cross section (σ_{GT}), $F=I_t/I_o$ determines the positronium-formation cross section (σ_{Ps}), while the partitioning of the Ps formation cross section from the grand total cross section, $\sigma_{(GT-Ps)}$, can also be experimentally determined using $F=I_m/I_t$.

For helium, the lowest energy threshold for electronic excitation by positrons is at a higher energy than the threshold for ground-state positronium formation. Therefore there exists an energy region, referred to as the Ore gap, in the grand total cross section, where the only two channels that are open are the elastic and positronium formation channels. On a technical note, one can effectively neglect the contribution of the positron-electron annihilation cross section since it is typically 5 orders of magnitude smaller than the elastic cross section above the Ps threshold. The Ore gap region for helium lies between 17.8 eV, the Ps formation threshold, and 20.6 eV, the He(2^1S) excitation threshold. Note that the 2^3S state at 19.8 eV cannot be excited by positrons as it requires a spin-flip transition, driven either by exchange or spin-orbit interactions. Therefore, within the Ore gap region,

$$\sigma_{(GT-Ps)} = \sigma_{el} \quad \text{for} \quad 17.8 \text{ eV} \le E \le 20.6 \text{ eV}, \tag{3}$$

where σ_{el} refers to the elastic cross section.

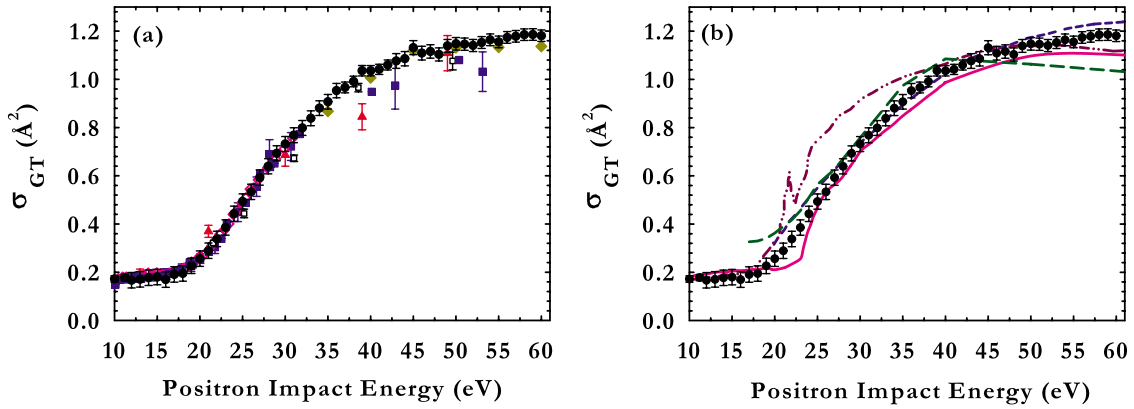

FIG. 3. (Color online) (a): Present grand total cross section (●) and the experimental results of Brenton *et al.* [6] (▲), Kauppila *et al.* [9] (♦), Canter *et al.* [7] (■), Stein *et al.* [10] (◇), and Coleman *et al.* [8] (□). (b): Present grand total cross section (●) compared with theoretical calculations of Baluja *et al.* [18] (– – –), Cheng *et al.* [19](— —) Campbell *et al.* [20] (-·-·-) and present CCC from l_{max}=8 calculation (–) (see text).

III. CONVERGENT CLOSE-COUPLING THEORY

The positron-helium scattering problem is difficult to calculate due to its two-center nature. However, single-center unitary theories, such as the convergent close-coupling (CCC) method [13,14], can be applied with some success. The effect of virtual Ps formation on elastic scattering at low energies can be treated to convergence using positive-energy pseudostates [15]. Above the ionization threshold the positive-energy pseudostates have the effect of treating both the breakup and the Ps formation processes together, again allowing for convergent results that agree with experiment [16]. However, in the energy region above the Ps formation threshold and below the ionization threshold, the CCC calculations become problematic.

Here, we are interested in the intermediate energy regime that contains the three energy ranges discussed above. When Ps formation becomes an important aspect of the scattering process this manifests itself as very slow convergence in the CCC calculations with increasing target-space orbital angular momentum l_{max}. This is particularly evident near the problematic energy region. To obtain convergent results over most of the energy studied in this work we took l_{max}=8. A total of 178 states were coupled, leading to a maximum of 802 channels at the higher partial waves of the total orbital angular momentum. By contrast, for electron scattering, when interested in total cross sections, we typically have l_{max}=4 with around 80 states and a maximum of 300 channels [17].

At energies above the ionization threshold the positive-energy states treat the Ps formation and breakup channels collectively. We can utilize the knowledge of the importance of large l to treat Ps formation to make an estimate of the Ps-formation cross section separately. At an energy a little above the ionization threshold we know that excitation of the positive-energy pseudostates predominantly corresponds to Ps formation. This is because the breakup cross section is zero at threshold while the Ps-formation threshold is 6.8 eV lower. At the higher energies, the breakup cross section is dominated by excitation of P states (photoionization limit). Hence, if we subtract the cross sections for exciting the positive-energy states in the l_{max}=8 and the l_{max}=1 calculations, then we obtain a rough, but plausible, estimate of the Ps-formation cross section.

IV. RESULTS AND DISCUSSION

A. Grand total Cross Section σ_{GT}

Our results for the grand total cross section below the positronium formation threshold, where only elastic scattering is possible, have been presented previously [11], so this paper will only focus on impact energies between 10 and 60 eV. For reasons of clarity, Fig. 3(a) only compares a selection of previous experimental measurements with the present grand total cross-section data. As can be seen, very good agreement exists between the present data and other experimental results [6–10].

Figure 3(b) compares a range of theoretical calculations with the present grand total measurements and indicates good overall agreement between experiment, and most theories presented [18,19]. The experimental cross section increases smoothly from low to high impact energies and shows no sign of the features present in the coupled-state method of Campbell *et al.* [20], which predicts the existence of a resonance-like spike near 22.5 eV, in the vicinity of the He(2^1S) and $Ps(n=2)$ states with thresholds at 20.6 and 22.9 eV, respectively.

Comparison between the present calculation and measurement shows very good agreement with the present results, with the exception of the above-mentioned problematic energy region between the positronium formation (17.8 eV) and the direct ionization (24.6 eV) thresholds, where the theory underestimates the experimental values. Interestingly, though not shown in the figure, comparison with smaller l_{max} calculations demonstrates that even the very large l_{max}=8 calculations are still not convergent in this energy range.

B. Positronium-formation cross section σ_{Ps}

Figure 4(a) shows that previous measurements for the positronium-formation cross section [21–25] are in good

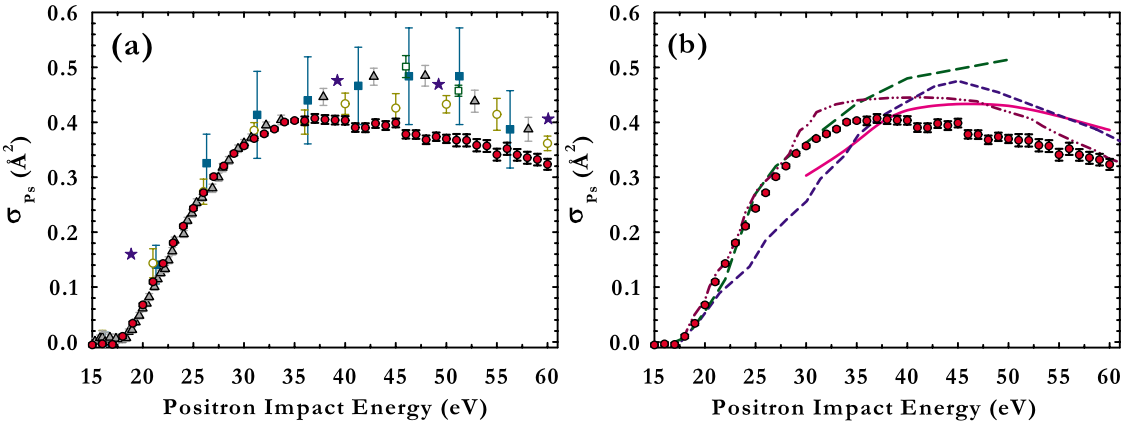

FIG. 4. (Color online) (a): Comparison between present positronium-formation cross section results (●), and those of Murtagh *et al.* [23] (▲), Overton *et al.* [21] (★), Fromme *et al.* [24] (○), Diana *et al.* [25] (□), and Fornari *et al.* [22] (■). (b): Present positronium-formation cross section results (●) compared with theoretical calculations of Cheng *et al.* [19](— —), Campbell *et al.* [20] (-·-·-·), McAlinden *et al.* [27] (– – –), and present CCC theory (–).

agreement with the present data below 37 eV, but disagree at higher energies, where the previous measurements predict higher cross section values compared to the data presented in this paper.

The disagreement between the present results and those of Murtagh *et al.* [23] is similar to that reported for the Ps formation cross measurements in the heavier rare gases by Marler *et al.* [26], who used the same experimental techniques as presented in this study. The Murtagh *et al.* Ps formation cross section results were derived by subtracting a measured direct ionization cross section from a measured total ionization cross section. Marler *et al.* speculated that the disagreement arose from an underestimation of the direct ionization cross section measured by Murtagh *et al.*, at higher energies, and were able to show agreement with the Murtagh *et al.* data when they used their own direct ionization measurements instead. Such an explanation may be applicable in this case, although there are no other absolute measurements of the direct ionization cross section available for positron scattering from helium. These measurements are scheduled to be performed by our group in the near future and we anticipate that these results could shed further light on this disagreement.

In the case of the other, older, studies of the Ps formation from helium, the source of the disagreement is not clear. Two of the previous measurements Overton *et al.* [21] and Diana *et al.* [25] used an attenuation method, similar in technique to that used here, but performed with a much weaker magnetic field, while Fromme *et al.* [24] used a similar method to Murtagh *et al.* While these measurements were very difficult, using low-strength positron beams with relatively poor-energy resolution, the origin of any discrepancies with the present measurements is not yet clear.

Comparison of the measured Ps formation cross section with previous theoretical calculations, in Fig. 4(b), suggests quantitative agreement at the 30% level. As was evident in the case of the total cross section, [Fig. 4(a)], the theoretical calculation of Campbell *et al.* [20] agrees well in shape, but predicts higher cross section values between 33 and 60 eV, when compared to the present results. Substantial discrepancies with the other theories exist, especially that of McAlinden *et al.* [27], and this is indicative of the challenges faced by theoreticians when calculating the Ps formation channel.

In the case of the present calculation, as described above, the Ps formation cross section starts with a magnitude, which is a little below the experimental results, at low energies, and ends up a little higher at the higher energies. At the lower energies it is difficult for all $l \leq l_{\max}$ pseudostates to adequately discretize the small positive-energy region. In principle, we could get more accurate CCC results here if we additionally increase the number of states for each l. However, given the approximate nature of the procedure this is not worth the computational expense.

C. Measurements in the region of the positronium, excitation, and ionization thresholds

The behavior of the scattering cross sections in the Ore gap region has been the subject of considerable speculation in the past. Campeanu *et al.* [28] suggested the possibility of channel coupling effects at the onset of positronium formation, due to a reported cusp-like feature, which appeared in the cross section that they derived for elastic scattering.

As discussed above, the present technique allows us to directly measure the grand total minus positronium-formation $\sigma_{(GT-Ps)}$ cross section. For energies below the first inelastic threshold, this corresponds to the total elastic cross section. Figure 5(a) shows the broad energy behavior of this cross section between 10 and 60 eV. Above the first excitation threshold, it shows a similar behavior to the grand total cross section, rising steadily through the impact energy range. There is some evidence of a feature just beyond the Ps formation threshold. Figure 5(b) reveals a detailed picture of this cross section in the region of the Ps, inelastic, and ionization thresholds, measured using 50 meV energy increments. As can be seen, the magnitude of the total elastic cross section through the Ore gap shows a definite, if small, dip between the Ps formation and 2^1S excitation threshold, which is not present in the calculations of Varrachio [29]. While this can be taken as evidence of channel coupling

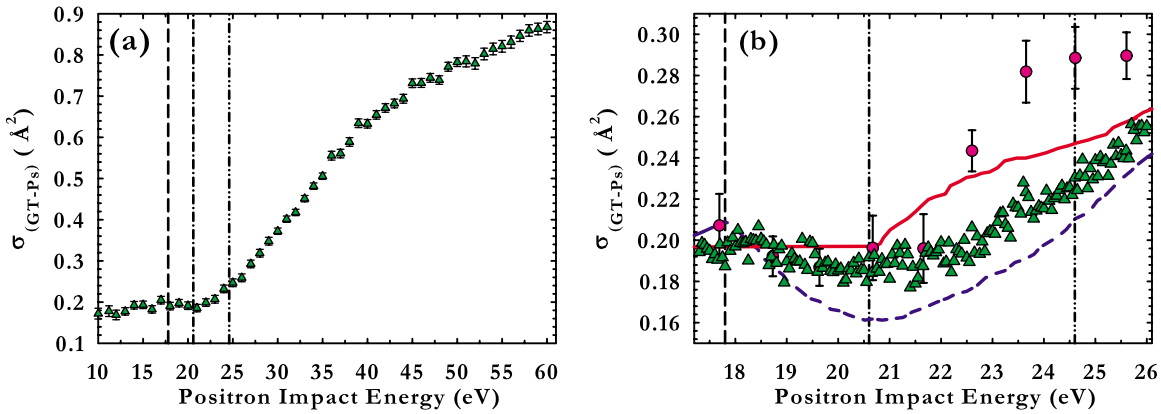

FIG. 5. (Color online) (a): Broad range energy behavior of the present grand total minus the positronium-formation cross section (▲) and (b): Comparison with calculations of Campeanu *et al.* [28] (– –), the random phase approximation of Varrachio [29] (—), and the experimental results of Coleman *et al.* [30] (●). The onset for Ps formation, excitation and direct ionization channels are indicated by (– –), (-·), and (-··) vertical lines, respectively.

effects, it is not as large as the effect calculated be Campeanu *et al.* [28]. The measurements compare favorably with those of Coleman *et al.* [30] up to the excitation threshold, confirming their conclusion that channel coupling effects are small in this region. However above 22 eV, the present results deviate from those of Coleman *et al.*, who claimed that a step in their data may be due to the onset of the electronic excitation cross section.

Previous measurements of the helium electronic excitation cross section by Coleman *et al.* [31,32], indicated a magnitude that is somewhat smaller than might be expected from the "step" in their elastic scattering measurements, as shown in Fig. 5(b). However, the measurements were reported as a lower bound on the total excitation cross section, and are, thus, not inconsistent with the step seen in their data. In the present measurement, the electronic excitation onset does not appear to affect the total nonpositronium-formation cross section in the manner suggested by Coleman *et al.* [30]. Measurements of the electronic excitation cross sections are underway in our laboratory and may shed further light on this question.

Figure 6 displays detailed measurements of the grand total and Ps formation cross sections in the region of the Ps, electronic excitation, and ionization thresholds. No observable features are detected in the spectra at this scale, and both cross sections rise smoothly through the threshold regions. These measurements were undertaken to explicitly search for the presence of scattering "resonances," which might occur if a positron temporarily binds to the helium atom. Similar negative-ion resonances are ubiquitous in electron scattering and are often observed at or near the opening of a new scattering channel. No such features have been observed to date in positron scattering cross sections. The notable exception are the features seen in the annihilation cross section for molecules at very low energies, which have been interpreted as vibrational Feshbach resonances [33,34].

Table I gives the current numerical values for the σ_{GT}, $\sigma_{(GT-Ps)}$ and the σ_{Ps}.

V. CONCLUSION

This paper presents absolute experimental measurements of the grand total, grand total minus Ps formation, and the Ps formation cross sections for positrons scattered by helium within the impact energy range of 10 to 60 eV. In addition, theoretical calculations of the grand total and Ps formation cross sections are also presented. A detailed investigation of the regions encomposing the Ps, excitation, and direct ionization thresholds using 50 meV energy increments has also been presented are presented. The typical energy resolution used to acquire these measurements was ~70 meV with absolute errors of ≤10%.

The present grand total cross section measurements are in good quantitative agreement across the entire impact energy range with previous experimental results, and in reasonable agreement with the theoretical predictions of [18,19]. The calculated grand total cross section presented in this paper, Fig. 3(b), shows overall agreement with present experimental results to ±10%, except for the region between the Ps formation (17.8 eV) and the direct ionization (24.6 eV) thresholds, where theory underestimates the contribution due to the Ps formation channel.

Quantitative agreement between the present Ps formation cross section measurements and previous experimental results is limited to the region between threshold to just below

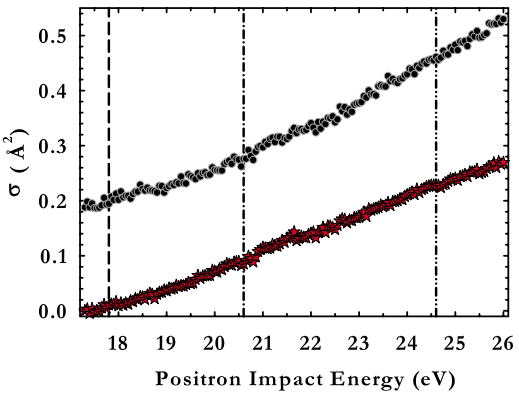

FIG. 6. (Color online) Fine threshold measurements of the present grand total (●) and positronium-formation (★) cross section using 50 meV energy steps. The onset for Ps formation, excitation, and direct ionization channels are indicated by (– –), (-·), and (-··) vertical lines, respectively.

TABLE I. Cross section data in units of ($Å^2$)

(ev)	σ_{GT}	$\Delta\sigma_{GT}$	$\sigma_{(GT-Ps)}$	$\Delta\sigma_{(GT-Ps)}$	σ_{Ps}	$\Delta\sigma_{Ps}$
10.0	0.172	0.013	0.172	0.013		
11.2	0.178	0.013	0.178	0.013		
12.0	0.167	0.032	0.169	0.012	0.000	0.003
13.0	0.170	0.032	0.177	0.009	−0.001	0.003
14.0	0.177	0.032	0.192	0.009	−0.005	0.003
15.0	0.180	0.032	0.193	0.009	−0.005	0.003
16.0	0.169	0.032	0.182	0.009	−0.003	0.003
17.0	0.191	0.032	0.205	0.009	−0.004	0.003
18.0	0.195	0.032	0.190	0.009	0.010	0.003
19.0	0.227	0.032	0.197	0.009	0.034	0.003
20.0	0.256	0.032	0.191	0.009	0.068	0.003
21.0	0.289	0.032	0.185	0.009	0.110	0.003
22.0	0.338	0.032	0.199	0.009	0.143	0.003
23.0	0.386	0.032	0.207	0.009	0.180	0.003
24.0	0.442	0.032	0.232	0.009	0.211	0.003
25.0	0.493	0.032	0.247	0.009	0.243	0.003
26.0	0.533	0.032	0.259	0.009	0.272	0.003
27.0	0.593	0.032	0.293	0.009	0.301	0.003
28.0	0.639	0.031	0.319	0.009	0.320	0.003
29.0	0.693	0.031	0.348	0.009	0.343	0.003
30.0	0.732	0.031	0.372	0.008	0.357	0.003
31.0	0.768	0.031	0.401	0.008	0.370	0.003
32.0	0.798	0.031	0.418	0.008	0.379	0.003
33.0	0.838	0.031	0.451	0.008	0.388	0.003
34.0	0.881	0.031	0.482	0.008	0.400	0.003
35.0	0.907	0.030	0.506	0.008	0.403	0.003
36.0	0.953	0.030	0.555	0.011	0.403	0.008
37.0	0.966	0.022	0.561	0.010	0.407	0.008
38.0	0.991	0.022	0.589	0.010	0.405	0.008
39.0	1.036	0.022	0.634	0.011	0.404	0.008
40.0	1.036	0.021	0.633	0.010	0.403	0.008
41.0	1.042	0.021	0.655	0.010	0.390	0.008
42.0	1.060	0.021	0.671	0.010	0.390	0.008
43.0	1.076	0.031	0.682	0.011	0.398	0.008
44.0	1.086	0.030	0.694	0.011	0.394	0.008
45.0	1.131	0.029	0.731	0.011	0.399	0.008
46.0	1.109	0.029	0.732	0.011	0.378	0.008
47.0	1.115	0.028	0.744	0.011	0.378	0.008
48.0	1.103	0.027	0.739	0.010	0.368	0.008
49.0	1.139	0.027	0.771	0.011	0.374	0.008
50.0	1.148	0.026	0.783	0.011	0.370	0.007
51.0	1.146	0.025	0.784	0.013	0.367	0.011
52.0	1.140	0.025	0.779	0.014	0.367	0.011
53.0	1.153	0.025	0.802	0.014	0.358	0.011
54.0	1.164	0.024	0.815	0.014	0.357	0.011
55.0	1.155	0.024	0.821	0.014	0.341	0.011
56.0	1.174	0.024	0.831	0.015	0.352	0.011
57.0	1.178	0.024	0.846	0.014	0.341	0.011

TABLE I. (*Continued.*)

(ev)	σ_{GT}	$\Delta\sigma_{GT}$	$\sigma_{(GT-Ps)}$	$\Delta\sigma_{(GT-Ps)}$	σ_{Ps}	$\Delta\sigma_{Ps}$
58.0	1.185	0.024	0.859	0.014	0.335	0.011
59.0	1.186	0.024	0.863	0.014	0.332	0.011
60.0	1.181	0.024	0.868	0.014	0.323	0.010

40 eV [Fig. 4(a)]. Results show that the absolute value of the Ps formation cross section is, in some cases, 20% smaller and reaches a maximum value around 10 eV below what was reported previously [24,25]. Comparison with theoretical calculations, shown in Fig. 4(b), reveals fair agreement with current Ps formation cross section results, and scope for improving the calculations using current techniques appear to be limited. This demonstrates the difficulty of accurate inclusion of the Ps formation channel into the calculations.

The present results also show some evidence of a broad, cusp-like feature in the elastic cross section at the Ps formation threshold, 17.8 eV, although it is much smaller than the prediction of Campeanu *et al.* [28]. No evidence was seen of the sharp rise in the $\sigma_{(GT-Ps)}$ cross section at the onset of the excitation threshold at 20.6 eV, which was attributed by Coleman *et al.* [30] to be due to the opening of the excitation channel. Indeed, the detailed measurements reveal that the $\sigma_{(GT-Ps)}$ cross section rises at a relatively constant rate, at least to the upper limit of the experimental measurement. The partitioning of the electronic and ionization cross sections is currently being investigated, and it is hoped that measurements of these cross sections will be published in the near future.

ACKNOWLEDGMENTS

The authors wish to acknowledge the funding of the Australian Research Council's Centre of Excellence Program. C.M. and J.P.S. also gratefully acknowledge the Australian Research Council for financial support. We are also indebted to Graeme Cornish, Stephen Battisson, Ross Tranter, and Ron Cruikshank for their excellent technical skills and ongoing support. We are grateful for access to the Australian Partnership for Advanced Computing and its Western Australian node iVEC.

[1] C. M. Surko, G. F. Gribakin, and S. J. Buckman, J. Phys. B **38**, R57 (2005).
[2] T. J. Murphy and C. M. Surko, Phys. Rev. A **46**, 5696 (1992).
[3] S. J. Gilbert, C. Kurz, R. G. Greaves, and C. M. Surko, Appl. Phys. Lett. **70**, 1944 (1997).
[4] J. P. Sullivan, S. J. Gilbert, J. P. Marler, R. G. Greaves, S. J. Buckman, and C. M. Surko, Phys. Rev. A **66**, 042708 (2002).
[5] T. Mizogawa, Y. Nakayama, T. Kawaratani, and M. Tosaki, Phys. Rev. A **31**, 2171 (1985).
[6] A. G. Brenton, J. Dutton, F. M. Harris, R. A. Jones, and D. M. Lewis, J. Phys. B **10**, 2699 (1977).
[7] K. F. Canter, P. G. Coleman, T. C. Griffith, and G. R. Heyland, J. Phys. B **6**, L201 (1973).
[8] P. G. Coleman, J. D. McNutt, L. M. Diana, and J. R. Burciaga, Phys. Rev. A **20**, 145 (1979).
[9] W. Kauppila (private communication).
[10] T. S. Stein, W. E. Kauppila, V. Pol, J. H. Smart, and G. Jesion, Phys. Rev. A **17**, 1600 (1978).
[11] J. P. Sullivan, C. Makochekanwa, A. Jones, P. Caradonna, and S. J. Buckman, J. Phys. B **41**, 081001 (2008).
[12] J. P. Sullivan, A. Jones, P. Caradonna, C. Makochekanwa, and S. J. Buckman, Rev. Sci. Instrum. **79**, 113105 (2008).
[13] I. Bray and A. T. Stelbovics, Phys. Rev. A **46**, 6995 (1992).
[14] D. V. Fursa and I. Bray, Phys. Rev. A **52**, 1279 (1995).
[15] H. Wu, I. Bray, D. V. Fursa, and A. T. Stelbovics, J. Phys. B **37**, L1 (2004).
[16] H. Wu, I. Bray, D. V. Fursa, and A. T. Stelbovics, J. Phys. B **37**, 1165 (2004).
[17] I. Bray, Phys. Rev. Lett. **73**, 1088 (1994).
[18] K. L. Baluja and A. Jain, Phys. Rev. A **46**, 1279 (1992).
[19] Y.-J. Cheng and Y.-J. Zhou, Chin. Phys. Lett. **24**, 3408 (2007).
[20] C. P. Campbell, M. T. McAlinden, A. A. Kernoghan, and H. R. J. Walters, Nucl. Instrum. Methods Phys. Res. B **143**, 41 (1998).
[21] N. Overton, R. J. Mills, and P. G. Coleman, J. Phys. B **26**, 3951 (1993).
[22] L. S. Fornari, L. M. Diana, and P. G. Coleman, Phys. Rev. Lett. **51**, 2276 (1983).
[23] D. J. Murtagh, M. Szluinska, J. Moxom, P. Van Reeth, and G. Laricchia, J. Phys. B **38**, 3857 (2005).
[24] D. Fromme, G. Kruse, W. Raith, and G. Sinapius, Phys. Rev. Lett. **57**, 3031 (1986).
[25] L. M. Diana, P. G. Coleman, D. L. Brooks, P. K. Pendleton, and D. M. Norman, Phys. Rev. A **34**, 2731 (1986).
[26] J. P. Marler, J. P. Sullivan, and C. M. Surko, Phys. Rev. A **71**, 022701 (2005).
[27] M. T. McAlinden and H. R. J. Walters, Hyperfine Interact. **73**, 65 (1992).
[28] R. I. Campeanu, D. Fromme, G. Kruse, R. P. McEachran, L. A. Parcell, W. Raith, G. Sinapius, and A. D. Stauffer, J. Phys. B **20**, 3557 (1987).
[29] E. F. Varracchio, J. Phys. B **23**, L779 (1990).
[30] P. G. Coleman, K. A. Johnston, A. M. G. Cox, A. Goodyear, and M. Charlton, J. Phys. B **25**, L585 (1992).
[31] P. G. Coleman and J. T. Hutton, Phys. Rev. Lett. **45**, 2017 (1980).
[32] P. G. Coleman, J. T. Hutton, D. R. Cook, and C. A. Chandler, Can. J. Phys. **60**, 584 (1982).
[33] L. D. Barnes, S. J. Gilbert, and C. M. Surko, Phys. Rev. A **67**, 032706 (2003).
[34] S. J. Gilbert, L. D. Barnes, J. P. Sullivan, and C. M. Surko, Phys. Rev. Lett. **88**, 043201 (2002).